bioresources.com

Preliminary Study of Laminated Glass with Nanocellulose and Poly(vinyl butyral) for Safety Glazing

Chloé Maury,[a] Frank Crispino,[b,c] and Éric Loranger [a,*]

The increase in fatal road accidents, natural disasters, and even terrorist attacks around the world have contributed to the improvement of public security. Windows can be particularly hazardous because of cutting fragments expelled during breakage or an explosion, which may induce injury. It is becoming essential to develop a resistant daily security glazing for houses to prevent damage in earthquakes and tornado areas, for utility cars, *etc*. Nanocellulose was used, which has a low ecological footprint, to improve safety glazing properties and was based on poly (vinyl butyral) (PVB). Following the processing of many different recipes for layers based on both PVB and nanocellulose polymers, intercalary films were assembled with glass using hot pressing. The results of the three-point bending experiments were promising. Breaking loads were approximately 8000 N for the two nanocellulose samples, which were close to the results of the sample with PVB only. Furthermore, the obtained composites possessed a transparency near that of PVB only. Finally, nanocellulose overtop PVB had a surface mass as low as one eighth of that of the PVB.

Contact information: a: Lignocellulosic Materials Research Center; b: Laboratoire de Recherche en Criminalistique; c: Centre International de Criminologie Comparée, Université du Québec à Trois-Rivières, 3351 Des Forges, Trois-Rivières, Québec G9A 5H7, Canada;
* Corresponding author: Eric.Loranger1@uqtr.ca

INTRODUCTION

Transparent safety glazing has a major role in various areas, such as the automobile industry, aerospace sector, building sector, and even in civil and military security. Currently, the increase in glass in buildings has led to new architectural requirements for the protection of the general public. In the near future, the demand for glass is expected to continue to increase, and protection requirements should integrate risks, such as natural disasters, uproar, and terrorist attacks (Xu *et al.* 2011; Zhang *et al.* 2013; Shim *et al.* 2015a). Furthermore, this kind of glass is particularly of interest for the automotive industries, specifically for windshields. In fact, during a collision between a car and a pedestrian, it is vital to prevent the release of glass fragments, which are responsible for physical injuries (Chen *et al.* 2016; Alter *et al.* 2017; Chen *et al.* 2017; Yu *et al.* 2017). To obtain resistant glazing, one or several poly (vinyl butyral) (PVB) interlayers are usually used between two (or several) glass sheets. This material adheres well to glass, is transparent, and absorbs energy upon impact (Zhang *et al.* 2013; Chang *et al.* 2014). Its adherence is caused by the presence of hydroxyl groups on the polymer skeleton after a butyraldehyde reaction in an acidic medium (Chang *et al.* 2014). Furthermore, this type of glazing possesses the characteristic of keeping broken pieces of glass in place. However, there are some notable problems. They are expensive, heavy,

thick, and possibly result in a loss of vision quality and transparency. Furthermore, long-term performance of adhesion between two annealed glasses is affected by an environmental phenomenon (stress corrosion) and by creep and relaxations phenomena. The last are due to external factors as UV-radiation, temperature, and humidity (Rodrigues *et al.* 2017). Indeed, Louter *et al.* (2010) showed the temperature greatly affected the structure of reinforced glass beams. One can then assume this problem will arise on safety glazing (Louter *et al.* 2010). Although it is known that long-term performance study of security glasses is of primary importance, this topic will be treated later. The raw material used for this type of polymer is petroleum, which is a polluting, non-degradable, and non-renewable material, and is likely to disappear in the coming years.

The challenge is to improve or maintain the transparency, while decreasing the weight and thickness. Nanocellulose seems to be an interesting alternative and it is used as a reinforcing agent in many polymeric matrices (Henriksson and Berglund 2007; Ahola *et al*. 2008; Rubentheren *et al*. 2016). Additionally, cellulose is renewable, recyclable, made from natural resources (Bertolla *et al*. 2014; Chang *et al*. 2014), and is the most abundant resource on Earth (Keijsers *et al*. 2013). This polymer is an advantage in the U.S. Green Building Council LEED® certification in Canada and the United States and in the Passive House Institute (PHI) standard in Europe. These certifications ensure that a contractor has done as much as possible to limit the ecological footprint of a building (PHI 2015; Canada Green Building Council 2018; U.S. Green Building Council 2018).

Nanocellulose is a long linear chain composed of many units of cellobiose, which contains two polysaccharide units (glucose) (Fig. 1). The selected wood species influences the degree of polymerization of the cellulose (Klemme *et al.* 2005; Ni *et al.* 2015). Cellulose possesses several properties and has a wealth of carboxylate groups on the surface of nanofibers, which makes it a promising material for addition in polymeric matrices (Venkatanarayanan and Stanley 2012; Li *et al.* 2014). Another interesting property for a security-glazing project is the optical characteristics of the nanocellulose because it is transparent, at least when used in the millimeter range normally used for glazing. In the literature, various applications have been developed because of this property, such as an organic light-emitting diode (Okahisa *et al.* 2009) and flexible optoelectronics sensors (Zhang *et al.* 2015b).
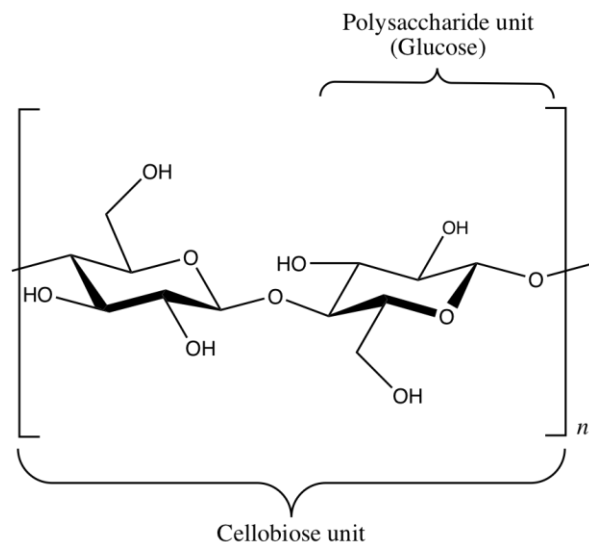
Fig. 1. Structure of the cellulose chain

Nanocellulose can be produced by selective oxidation with a TEMPO catalyzer under light ultrasound conditions (Rattaz *et al.* 2011; Mishra *et al.* 2012; Paquin *et al.* 2013). Currently, as this fabrication is well known, new applications are needed to fully exploit this material produced for security glazing. Nanocellulose manufactured by this process is of interest for this project because the fibers are longer (200 nm to several micrometers) than those of the popular cellulose nanocrystals, and surface modification is easier for retaining the amorphous region (Saito and Isogai 2006; Saito *et al.* 2007). Additionally, the presence of carboxylate groups on the surface of nanofibers allows TEMPO-oxidized cellulose gel (TOCgel) to be a good reinforcing agent in polymeric matrices (Venkatanarayanan and Stanley 2012; Li *et al.* 2014; Zhang *et al.* 2015a).

In the literature, several studies have shown that the relative density, laminate design, and stress fracture influence the ballistic resistance of a material (Nasirzadeh and Sabet 2014; Shim *et al.* 2015b). The glass and polymer densities are important factors that influence the protection performance (Shim *et al.* 2015b). In this study, part of the poly (vinyl butyral-co-vinyl, alcohol-co-vinyl acetate) (co-PVB) was replaced with either a cellulose composite or a cellulose and poly (vinyl alcohol) (PVOH) composite.

First, the Young's modulus of the interlayers was assessed (strain and elongation). Then, the load at break during the three-point bending tests was evaluated on laminated glass sheets with each type of interlayer.

EXPERIMENTAL

Materials

A co-PVB powder with an average molecular weight of 70,000 M_w to 100,000 M_w was purchased from Sigma Aldrich (St. Louis, MO, USA). The chemical composition of the co-PVB was 80 wt% vinyl butyral, 18 wt% to 20 wt% hydroxyl, and 0 wt% to 1.5 wt% acetate. A PVOH powder with an average molecular weight of 146,000 M_w to 186,000 M_w was also purchased from Sigma Aldrich and used without further purification. Pure ethanol was used for the co-PVB solution, while aqueous solutions

were prepared with deionized water ($\Omega < 0.8$ µS). Conventional 10-cm x 10-cm clear annealed glass sheets with a thickness 6 mm were purchased from a local supplier (Vitrerie Lambert et fils, Trois-Rivières, Québec, Canada).

A commercial never-dried bleached Kraft hardwood pulp was used as the cellulose source for the production of the TOCgel and nanocellulose through TEMPO oxidation and mechanical dispersion. All of the oxidation chemicals (TEMPO, sodium bromide, and sodium hypochlorite) were also purchased from Sigma Aldrich and used as received.

Methods

TOCgel preparation

First, 9.2 g of acetaminoTEMPO, 3.1 mmol/g of NaOCl, and 25 g of NaBr were mixed with a fibrous suspension of 1% kraft pulp, which corresponded to 400 g of dry pulp in 40 L of deionized water. The pH of the reaction was set at 10.5 and the temperature in the reactor was maintained at 25 °C. The acoustic frequency used in the pilot sonoreactor (Ultrasonic Power Corporation, Freeport, USA) was 170 kHz, and the power was 125 W. With these conditions (Rattaz *et al.* 2011; Mishra *et al.* 2012; Paquin *et al.* 2013), the nanofibers produced from the kraft pulp had a measured carboxyl content of 1700 mmol/kg. A mix of long microfibers (30%) and short nanofibers (70%) resulted in the TOCgel having an average width and length of approximately 3.5 mm ± 1.0 mm and 306 nm ± 112 nm, respectively.

Then, the TOCgel was manufactured by simple shearing with a MK 2000/4 refiner (defibrillation system) from IKA Works, Inc. (Wilmington, NC, USA). A 3% gel was obtained with an oxidized pulp of 1700 mmol/kg. The defibrillated oxidized pulp was placed in a plexiglass tank, which was connected to a pump, the IKA defibrillator, and a bubble cooler, for defibrillation. This process lasted 1 h (Loranger *et al.* 2012).

Nanocellulose preparation

The TOCgel produced was diluted by 50%, from a concentration of 2.5% to 1.25% (w/w), and then it was defibrillated a second time with the IKA defibrillator for 1 h. The obtained solution (50 mL) was centrifuged with a Thermo Scientific Sorvall ST16 (Waltham, MA, USA) centrifuge at 13000 rpm for 15 min. The supernatant, including pure nanocellulose, was retrieved and used as is.

Sheet layers preparation

For each interlayer, the same fabrication method was used. A prepared solution was poured into an aluminum cup (18 cm in diameter) and dried at ambient air temperature (23 °C). For the 2% co-PVB interlayers (PVB2), 2 g of co-PVB powder was dispersed in 100 mL of ethanol. For the nanocellulose interlayers, 300 mL of the 1.25% nanocellulose aqueous solution was poured into the cup. During the first tests, the pure nanocellulose films obtained were very brittle. It was then necessary to increase the cohesion of the fibers by the addition of another polymer, which allowed for a uniform film to be obtained. The authors chose to include PVOH, which is a water-soluble polymer that is easily miscible with nanocellulose. The solutions nanoPVOH$_{100}$ and nanoPVOH$_{50}$ were made with 300 mL of the 1.25% nanocellulose solution added to 100 mL of the 2% PVOH solution and 300 mL of the 1.25% nanocellulose solution added to 50 mL of the 2% PVOH solution, respectively. Finally, the last interlayers were made by means of 150 mL of the 2.5% TOCgel dispersed in 150 mL of deionized water (TOCgel).

Another interlayer was made with the further addition of 50 mL of the 2% PVOH solution (TOCgelPVOH) (Table 1 and Fig. 2a).

Table 1. Composition of Each Interlayer Based on the Cellulose and their Resulting Thickness and Geometry

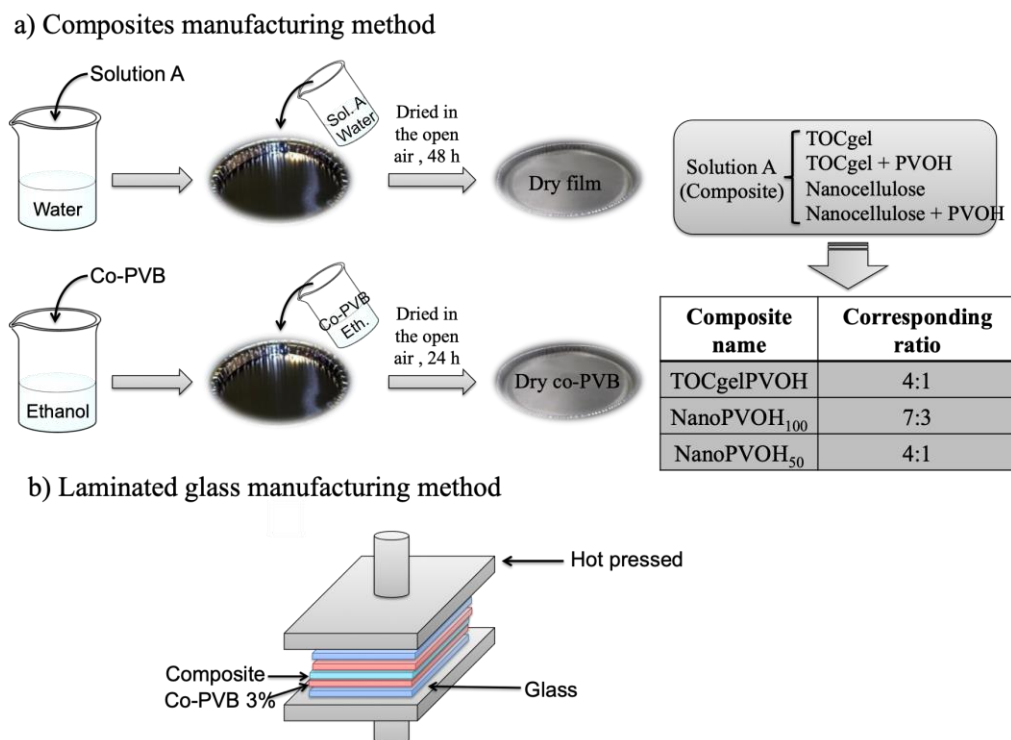| Sample	Composition Before Drying			Thickness After Drying (µm)	Geometry After Drying
	1.25% Nanocellulose Solution (mL)	2.5% TOCgel Solution (mL)	2% PVOH Solution (mL)		
Nanocellulose	300	---	---	10 ± 0.51	Fibers
NanoPVOH$_{100}$	300	---	100	60 ± 1.07	Fibers + thermoplastic
NanoPVOH$_{50}$	300	---	50	40 ± 0.47	Fibers + thermoplastic
TOCgel	---	150	---	30 ± 0.75	Fibers
TOCgelPVOH	---	150	50	70 ± 1.06	Fibers + thermoplastic

Fig. 2. Representative drawing of the (a) composite manufacturing method and (b) laminated glass manufacturing method

Glass and layer lamination

To produce the laminated glazing, another interlayer based on cellulose or PVB was included between two layers of 3% co-PVB to enable the addition of nanocellulose and PVOH to the glazing. This addition of co-PVB was necessary because the new interlayers based on cellulose and PVOH do not adhere to glass panes. In fact, adherence to the panes is one of the main advantages of PVB. Furthermore, two PVB interlayers and a new PVB interlayer were used to reach the lower thickness limit of existing PVB

interlayers (between 0.38 mm and 1.54 mm). The layers were then placed between two layers of glass (6 mm in thickness) and fused together by hot pressing. The assembly was hot-pressed for 30 min at 2 bar and a temperature of 110 °C (Fig. 2b).

Characterization

Thermogravimetric analysis of the layers

The thermogravimetric analysis enabled sample mass variations to be measured with respect to the applied temperature program. From this, the thermal degradation characteristics of the composites and control samples could be studied. The sample (approximately 5 mg) to be analyzed was placed in a cup on a precision scale. The same cup was then placed in an oven, which exposed the sample to a temperature program and continuously measured the change in the weight. The analyses were done using a Diamond Pyris TGA/DTA™ apparatus from Perkin-Elmer (Waltham, MA, USA). For the temperature program, the sample was first subjected to a temperature of 50 °C for 15 min to minimize the water content. Then, the sample was submitted to temperatures ranging from 50 °C to 575 °C with a heating rate of 5 °C/min under an inert atmosphere (nitrogen). Finally, the sample was heated from 575 °C to 750 °C at a rate of 10 °C/min in air to determine the total deterioration.

Tensile test of the layers

A tensile apparatus (Instron 4201™, Instron, Norwood, MA, USA) was used to measure the notched tensile strength of the pure TOCgel, pure co-PVB, and each sample. Stress/strain curves were used to determine the elongation at break and Young's modulus of all of the composites. A film 16 mm in length and 8 mm in width with a thickness between 0.05 mm and 0.30 mm was produced for each sample. A 0.5-cm linear notch on each side at 8 mm along the length was made to guarantee a proper break at the mid-length of each sample. This test method used a head speed displacement rate of 10 mm/min and a load cell of 500 N. The reported results were the average of the measurements taken of 15 samples.

Three-point bending test of the glazing

Three-point bending tests of the glazing of the pure TOCgel, pure co-PVB, and each composite layer were conducted on an Instron 4201™ apparatus at room temperature. The load at break and Young's modulus of each sample were determined with the stress/strain curves. Each sample was 10 cm in length and width and 12 mm in thickness. This method used a rate of 2 mm/min and a force cell of 5 kN. For each composite, three measurements were taken and the average was reported. Some samples did not break before the 5-kN apparatus limit was reached. It was then necessary to use the Instron LM-U150™ apparatus (Instron) equipped with a 25-kN load cell. Except for changing to a device with a larger force cell, the same method described previously was used.

Light transmission of the composites interlayers and glazing

A Tint Meter Inspector Model 200™ (Laser Labs, Inc., Scituate, MA, USA) was used to study the light transmission. The Canadian police force uses this apparatus to enforce various laws concerning the maximum vehicle window tint. A minimum of 70% of light must pass through vehicle windows under Quebec regulations (Société de

l'Assurance Automobile du Québec 2018; Vitro Plus 2018). In this study, the 70% minimum was used as a comparison base to determine whether the samples were usable. A receiver and transmitter, aligned using a powerful magnet, were placed at the base of the apparatus. Calibration was done automatically and double-checked with the help of standards that transmit 28% and 78% of light. The reading of the measurements was simple and instantaneous after placing the sample between the receiver and transmitter. Ambient light does not affect this device (Laser Labs Inc., 2018). For each sample, five different spots were measured and the average value was reported.

RESULTS AND DISCUSSION

Thermogravimetric Analysis

From the thermogravimetric analysis, two characteristics were observed: the presence of polymer in the composite materials and the degradation temperature. Table 2 and Fig. 3a show that the nanocellulose and TOCgel had similar degradation temperatures (approximately 260 °C); these results are consistent because their basic polymer composition is the same (cellulose). The two thermoplastics used in the project, co-PVB and PVOH, had degradation temperatures of 368.7 °C and 431.8 °C, respectively. Regarding the three composites containing cellulose and PVOH, which are shown in Fig. 3b, two degradation temperatures were obtained for each, at approximately 260 °C and 430 °C, respectively. These results confirmed that the manufactured films contain a mixture of the two polymers cellulose and PVOH. Also, it was observed that the PVOH had a degradation temperature above that of the co-PVB. The addition of PVOH to the films was an advantage in terms of the thermal properties. Finally, the mass loss of the $nanoPVOH_{100}$ composite was lower than that of the TOCgelPVOH and $nanoPVOH_{50}$ composites. After comparing the two similar composites ($nanoPVOH_{50}$ and $nanoPVOH_{100}$), it was observed that when there was more PVOH, the nanocellulose was less degraded at the same temperature. These results indicated the thermal efficiency of the PVOH (Fig. 3).

Table 2. Experimental Data of the Degradation Temperature for the Control Samples and Composites

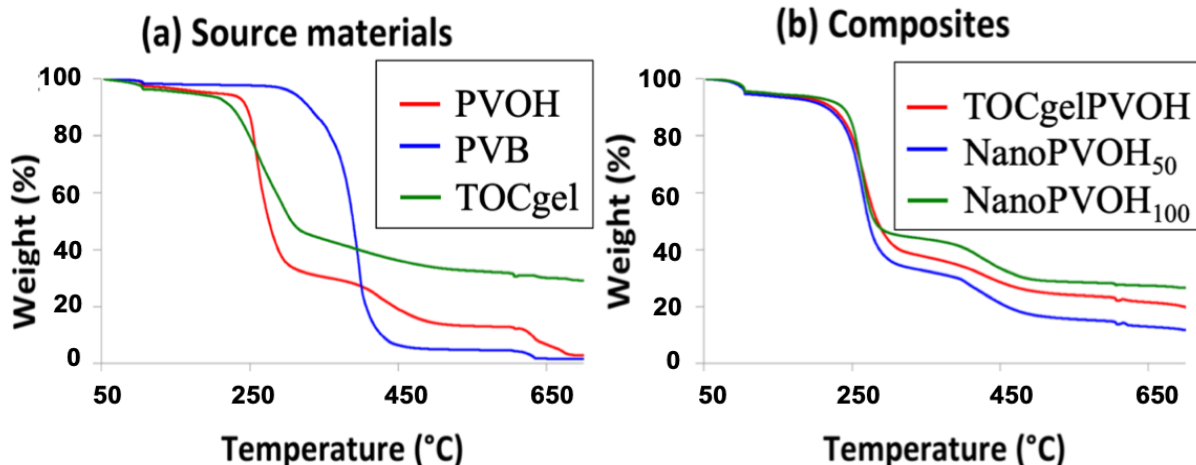| Sample	Nanocell.	TOCgel	Co-PVB	PVOH	TOCgel PVOH	Nano PVOH 100	Nano PVOH 50
Degradation Temperature (°C)	258.4	266.7	368.7	431.8	264.8 428.1	262.5 431.9	262.8 439.7

Fig. 3. Thermogravimetric analysis of (a) source materials and (b) composites

Tensile Testing of the Layered Composites

The tensile test results are presented in Figs. 4 and 5. The nanocellulose, TOCgel, and co-PVB control samples had a Young's modulus of 13 GPa ± 1.9 GPa, 4.4 GPa ± 0.4 GPa, and 1.3 GPa ± 0.1 GPa, respectively. These results indicated that the nanocellulose was the material with the most rigidity, whereas the co-PVB was the least rigid. Figure 5 shows the stress/strain curves, which confirmed that the elastic behavior of the co-PVB (light blue curve) had a typical curve related to this phenomenon, whereas the nanocellulose had a very rigid behavior with a straight line (green curve). Furthermore, the co-PVB was the most flexible with an elongation at break of 4.73% ± 2.37%. For the composite interlayers, the Young's moduli were similar for the three samples (TOCgelPVOH, NanoPVOH$_{100}$, and NanoPVOH$_{50}$) and the elongation at break was more important for the nanoPVOH$_{100}$ (3.06% ± 0.94%) than for the TOCgelPVOH and nanoPVOH$_{50}$ composites (approximately 2%). This phenomenon could have been explained by the presence of PVOH, which is a thermoplastic. Compared with the co-PVB, the currently used interlayer for safety glass composites has a Young's modulus that is at best approximately 4.5 times higher than that of the co-PVB, but it has half the elongation at break on average. The increase in the Young's modulus of the composites relative to that of the co-PVB was caused by the presence of a rigid cellulose matrix. The PVOH can solder the fibers between it because of its thermoplastic properties and play the role of a glue, which also explained the increase in the Young's modulus compared with that of the pure TOCgel. These results are consistent with that in the literature, where co-PVB has a Young's modulus of 1.93 GPa and tensile strength of 26 MPa (Shim *et al.* 2015a).
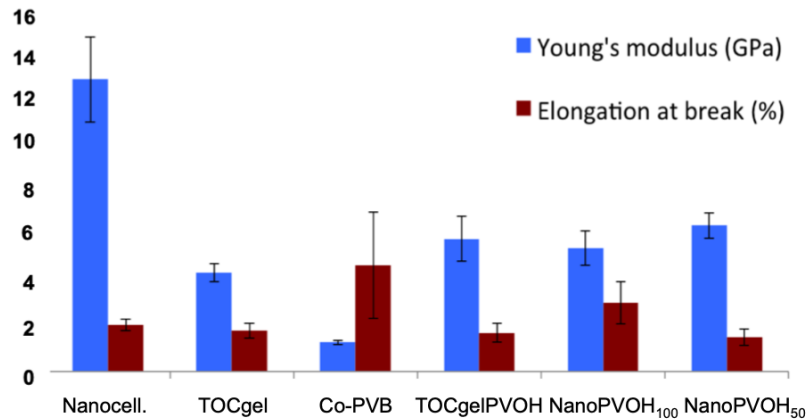
Fig. 4. Experimental data from the tensile tests on the control samples and composite films
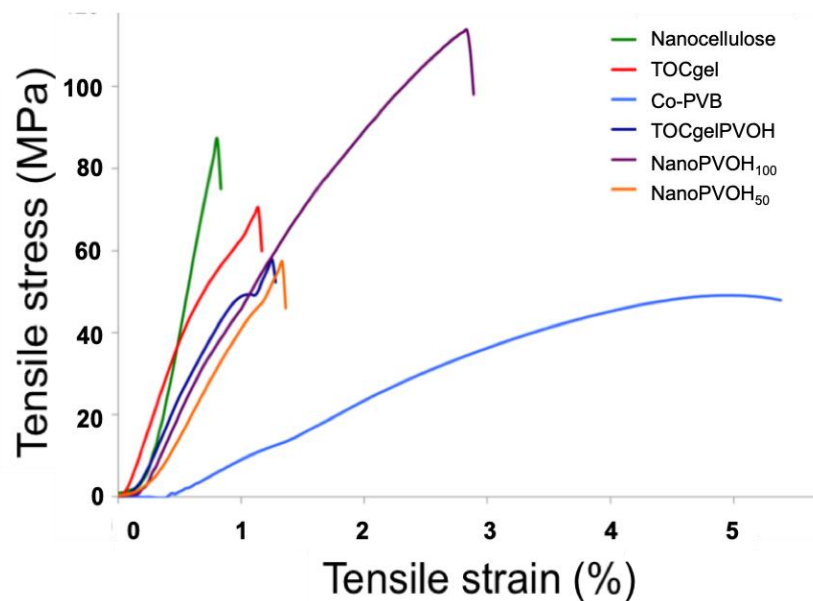

Fig. 5. Strain/stress curves of the control samples and composite films

Three-point Bending Testing of the Laminated Glazing

The load at break for the control samples and composites are shown in Figs. 6 and 7. Each sample had a Young's modulus of approximately 4 MPa, and so no specific comparison could be made. However, it should be noted in this part, as soon as we speak of samples, the latter correspond each time to full glazing (glasses + interlayers). In contrast, the loads at break of the co-PVB, nanoPVOH$_{50}$, and nanocellulose were approximately 8000 N, 7800 N, and 8000 N, respectively, which were better than that of glass alone (1800 N). These results showed a real improvement in the applied force required for breaking glass that had only interlayers made with the pure nanocellulose and nanoPVOH$_{50}$ composite. These results are particularly interesting because the co-PVB, nanoPVOH$_{50}$, and nanocellulose mass per unit area were 0.086 kg/m^2, 0.048 kg/m^2, and 0.012 kg/m^2, respectively. The loads at break of the nanocellulose and nanoPVOH$_{50}$ might have been only slightly improved over that of the co-PVB, but their mass per unit areas were one-eighth and one-half that of the co-PVB, respectively.
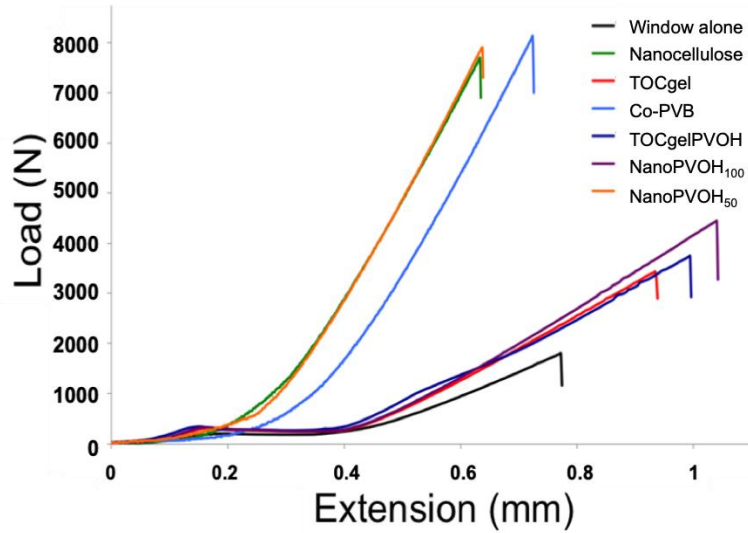
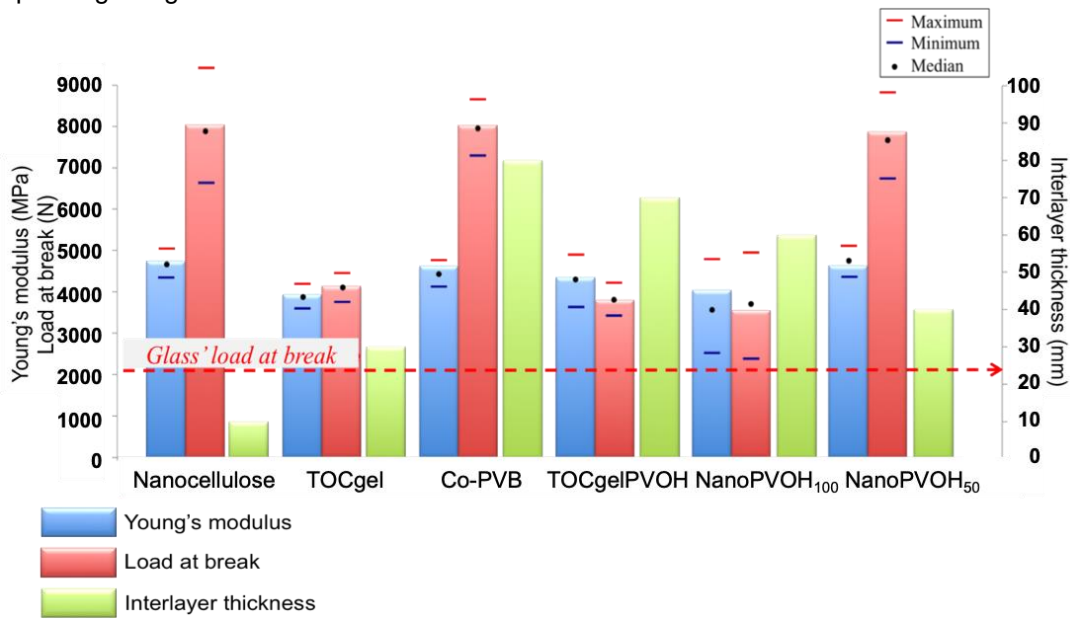**Fig. 6.** Experimental data from the three-point bending tests on the control samples and composite glazing

Fig. 7. Experimental data from the three-point bending tests on the control samples and composite films

Light Transmission of the Laminated Glazing

The light transmission results of the laminated and interlayer composites are shown in Table 3. In terms of the light transmission of the composites without glass, the co-PVB film had a transmission of 93%, which was similar to that of the nanocellulose, nanoPVOH$_{100}$ composite, and nanoPVOH$_{50}$ composite. The TOCgel had a transmission of only 82% and the TOCgelPVOH composite had a transmission of 87%. This phenomenon was explained by the presence of long fibers in the TOCgel, which can diffract light. However, these fibers were removed by centrifugation in the nanocellulose solutions, which improved the light transmission. These results were interesting because the co-PVB and many composites had the same light transmission. For the glazing, the

laminated glass with co-PVB had a light transmission of 80% with an interlayer that was 80 µm in thickness, which was because of the experimental synthesis conditions. Except for the TOCgel (68%) and TOCgelPVOH (67%), all of the samples had light transmissions similar to that of the co-PVB and were between 75% and 80%, but they had a reduced interlayer thickness. (Shim *et al.* 2015b) found that the light transmission of laminated glass was approximately 80%, so it was inferred that it is possible to use the laminated glass as transparent bulletproof materials. Furthermore, the optical properties should be considered during the designing of bulletproof materials (Shim *et al.* 2015b).

Table 3. Light Transmission and Thickness of the Control Samples and Composites with and without Glass

Sample/Intercalary	Material Light Transmission (%)	Laminated Glass Light Transmission (%)	Film Thickness (µm)
Nanocellulose	93	79	10 ± 0.51
TOCgel	82	68	30 ± 0.75
Co-PVB	93	80	80 ± 0.30
TOCgelPVOH	87	67	70 ± 1.06
NanoPVOH$_{100}$	93	76	60 ± 1.07
NanoPVOH$_{50}$	93	78	40 ± 0.47

CONCLUSIONS

1. The Young's modulus was four times higher and the elongation at the break was approximately half that of the co-PVB for the three composites TOCgelPVOH, nanoPVOH$_{100}$, and nanoPVOH$_{50}$. The cellulose acted as a good reinforcement for the co-PVB and only a small loss of elasticity was observed.

2. The nanocellulose and nanoPVOH$_{50}$ interlayers performed notably well when they were applied in a glazing and had loads at break larger than for the co-PVB (approximately 8000 N) and laminated sheets with a lower mass per unit area.

3. A good light transmission was observed for the composites with nanocellulose, close to 80%, which is above the legal limit for motor vehicles.

4. The addition of PVOH resulted in a decrease in the load at break, but improved the thermal degradation by 60 °C.

5. The laminated glass produced in this study can have many applications in various fields, such as the building, civil and military, automobile, and aerospace sectors.

ACKNOWLEDGMENTS

bioresources.com

REFERENCES CITED

Ahola, S., Österberg, M., and Laine, J. (2008). "Cellulose nanofibrils-adsorption with poly(amideamine) epichlorohydrin studied by QCM-D and application as a paper strength additive," *Cellulose* 15(2), 303-314. DOI: 10.1007/s10570-007-9167-3

Alter, C., Kolling, S., Schneider, J. (2017). "An enhanced non-local failure criterion for laminated glass under low velocity impact," *International Journal of Impact Engineering*. 109, 342-353. DOI: 10.1016/j.ijimpeng.2017.07.014

Bertolla, L., Dlouhý, I., and Boccaccini, A. R. (2014). "Preparation and characterization of Bioglass®-based scaffolds reinforced by poly-vinyl alcohol/microfibrillated cellulose composite coating," *J. Eur. Ceram. Soc.* 34(14), 3379-3387. DOI: 10.1016/j.jeurceramsoc.2014.04.003

Canada Green Building Council (2018). "About us," (http://www.cagbc.org/CAGBC/About/CAGBC/AboutCaGBC/About_CaGBC.aspx?hkey=2259347d-6d16-4417-ba6c-a442711f95a1), Accessed 27 April 2016.

Chang, C., Teramoto, Y., and Nishio, Y. (2014). "High performance films of cellulose butyral derivative having a necklace-like annular structure in the side chains," *Polymer* 55(16), 3944-3950. DOI: 10.1016/j.polymer.2014.06.087

Chen, S., Zang, M., Wang, D., Zheng, Z. and Zhao, C. (2016). "Finite element modeling of impact damage in polyvinyl butyral laminated glass," *Composite Structures*. 138, 1-11. DOI: 10.1016/j.compstruct.2015.11.042

Chen, S., Zang, M., Wang, D., Yoshimura, S., and Yamada, T. (2017). "Numerical analysis of impact failure of automotive laminated glass: A review," *Composites Part B: Engineering*. 122, 47-60. DOI: 10.1016/j.compositesb.2017.04.007

Henriksson, M., and Berglund, L. A. (2007). "Structure and properties of cellulose nanocomposite films containing melamine formaldehyde," *J. Appl. Polym. Sci.* 106(4), 2817-2824. DOI: 10.1002/app.26946

Keijsers, E. R. P., Yılmaz, G., and van Dam, J. E. G. (2013). "The cellulose resource matrix," *Carbohyd. Polym.* 93(1), 9-21. DOI: 10.1016/j.carbpol.2012.08.110

Klemme, D., Heublein, B., Fink, H. P., and Bohn, A. (2005). "Cellulose: Fascinating biopolymer and sustainable raw material," *Angew. Chem. Int. Edit.* 44(22), 3358-3393. DOI: 10.1002/anie.200460587

Laser Labs Inc (2018). "Inspector tint meter model 200 user manual," (http://15203-presscdn-0-10.pagely.netdna-cdn.com/wp-content/uploads/2015/11/Laser-Labs-TM200-brochure-01a.png), Accessed 10 January 2016.

Li, W., Wu, Q., Zhao, X., Huang, Z., Cao, J., Li, J., and Liu, S. (2014). "Enhanced thermal and mechanical properties of PVOH composites formed with filamentous nanocellulose fibrils," *Carbohyd. Polym.* 113, 403-410. DOI: 10.1016/j.carbpol.2014.07.031

Loranger, L., Piché, A. O., and Daneault, C. (2012). "Influence of high shear dispersion on the production of cellulose nanofibers by ultrasound-assisted TEMPO-oxidation of kraft pulp," *Nanomaterials-Basel* 2(3), 286-297. DOI: 10.3390/nano2030286

Louter, C., Belis, J., Bos, F., Callewaert, D., Veer, F. (2010). "Experimental investigation of the temperature effect on the structural response of SG-laminated reinforced glass beams," *Engineering Structures* 32(6), 1590-1599. DOI: 10.1016/j.engstruct.2010.02.007

Mishra, S. P., Manent, A.-S., Chabot, B., and Daneault, C. (2012). "Production of nanocellulose from native cellulose - Various options utilizing ultrasound," *BioResources* 7(1), 422-436. DOI: 10.15376/biores.7.1.422-436

Nasirzadeh, R., and Sabet, A. R. (2014). "Study of foam density variations in composite sandwich panels under high velocity impact loading," *Int. J. Impact Eng.* 63, 129-139. DOI: 10.1016/j.ijimpeng.2013.08.009

Ni, J., Teng, N., Chen, H., Wang, J., Zhu, J., and Na, H. (2015). "Hydrolysis behavior of regenerated celluloses with different degree of polymerization under microwave radiation," *Bioresource Technol.* 191, 229-233. DOI: 10.1016/j.biortech.2015.05.036

Okahisa, Y., Yoshida, A., Miyaguchi, S., and Yano, H. (2009). "Optically transparent wood-cellulose nanocomposite as a base substrate for flexible organic light-emitting diode displays," *Compos. Sci. Technol.* 69(11-12), 1958-1961. DOI: 10.1016/j.compscitech.2009.04.017

Paquin, M., Loranger, É., Hannaux, V., Chabot, B., and Daneault, C. (2013). "The use of Weissler method for scale-up a kraft pulp oxidation by TEMPO-mediated system from a batch mode to a continuous flow-through sonoreactor," *Ultrason. Sonochem.* 20(1), 103-108. DOI: 10.1016/j.ultsonch.2012.08.007

PHI (2015). *Passive House Institute (PHI)*, (http://passivehouse.com), Accessed 27 April 2016.

Rattaz, A., Mishra, S. P., Chabot, B., and Daneault, C. (2011). "Cellulose nanofibers by sonocatalysed-TEMPO-oxidation," *Cellulose* 18(3), 585-593. DOI: 10.1007/s10570-011-9529-8

Rodrigues, T., Jordão, S., and Bedon, C. (2017). "Long-term effects on structural glass beams," *XI Congresso de Construção Metálica e Mista, CMM Press*, 933-942.

Rubentheren, V., Ward, T. A., Chee, C. C., Nair, P., Salami, E., and Fearday, C. (2016). "Effects of heat treatment on chitosan nanocomposite film reinforced with nanocrystalline cellulose and tannic acid," *Carbohyd. Polym.* 140, 202-208. DOI: 10.1016/j.carbpol.2015.12.068

Saito, T., and Isogai, A. (2006). "Introduction of aldehyde groups on surfaces of native cellulose fibers by TEMPO-mediated oxidation," *Colloid. Surface. A* 289(1-3), 219-225. DOI: 10.1016/j.colsurfa.2006.04.038

Saito, T., Kimura, S., Nishiyama, Y., and Isogai, A. (2007). "Cellulose nanofibers prepared by TEMPO-mediated oxidation of native cellulose," *Biomacromolecules* 8(8), 2485-2491. DOI: 10.1021/bm0703970

Shim, G.-I., Eom, H.-W., Kim, S.-H., Park, J.-K., and Choi, S.-Y. (2015a). "Fabrication of lightweight and thin bulletproof windows using borosilicate glass strengthened by ion exchange," *Compos. Part B-Eng.* 69, 44-49. DOI: 10.1016/j.compositesb.2014.09.023

Shim, G.-I., Kim, S.-H., Eom, H.-W., Ahn, D.-L., Park, J.-K., and Choi, S.-Y. (2015b). "Improvement in ballistic impact resistance of a transparent bulletproof material laminated with strengthened soda-lime silicate glass," *Compos. Part B-Eng.* 77, 169-178. DOI: 10.1016/j.compositesb.2015.03.035

Société de l'Assurance Automobile Québec (2018). "Vitres teintées," (https://saaq.gouv.qc.ca/securite-routiere/moyens-deplacement/auto/auto-modifiee/vitres-teintees/), Accessed 22 May 2017.

U.S. Green Building Council (2018). "LEED is green building," (http://www.usgbc.org/leed), Accessed 27 April 2016.

Venkatanarayanan, P. S., and Stanley, A. J. (2012). "Intermediate velocity bullet impact response of laminated glass fiber reinforced hybrid (HEP) resin carbon nano composite," *Aerosp. Sci. Technol.* 21(1), 75-83. DOI: 10.1016/j.ast.2011.05.007

Vitro Plus (2018). "Vitres teintées," (http://www.vitroplus.com/teintage-de-vitres.html), Accessed 22 May 2017.

Xu, J., Li, Y., Liu, B., Zhu, M., and Ge, D. (2011). "Experimental study on mechanical behavior of PVB laminated glass under quasi-static and dynamic loadings," *Compos. Part B-Eng.* 42(2), 302-308. DOI: 10.1016/j.compositesb.2010.10.009

Yu, G., Zheng, Y., Feng, B., Liu, B., Meng, K., Yang, X., Chen, H., and Xu, J. (2017). "Computation modeling of laminated crack glass windshields subjected to headform impact," *Computers & Structures*. 193, 139-154. DOI: 10.1016/j.compstruc.2017.08.011

Zhang, X., Hao, H., and Ma, G. (2013). "Parametric study of laminated glass window response to blast loads," *Eng. Struct.* 56, 1707-1717. DOI: 10.1016/j.engstruct.2013.08.007

Zhang, X., Hao, H., Shi, Y., and Cui, J. (2015a). "The mechanical properties of polyvinyl butyral (PVB) at high strain rates," *Constr. Build. Mater.* 93, 404-415. DOI: 10.1016/j.conbuildmat.2015.04.057

Zhang, Z., Wang, H., Li, S., Li, L., and Li, D. (2015b). "Transparent and flexible cellulose nanofibers/silver nanowires/acrylic resin composite electrode," *Compos. Part A-Appl. S.* 76, 309-315. DOI: 10.1016/j.compositesa.2015.06.010